RSC Advances

PAPER

View Article Online
View Journal | View Issue

Cite this: *RSC Adv.*, 2020, **10**, 44494

Non-swellable F127-DA hydrogel with concave microwells for formation of uniform-sized vascular spheroids†

Yingjun Li, Ying Wang, Chong Shen and Qin Meng *

Received 20th July 2020
Accepted 3rd November 2020

DOI: 10.1039/d0ra06188c

rsc.li/rsc-advances

Hydrogels with concave microwells are one of the simplest means to obtain uniform-sized cellular spheroids. However, the inherent swelling of hydrogels leads to reduced mechanical strength and thus deforms the structure of the microwells. In this study, we developed a hydrogel with microwells for formation of vascular spheroids *via* non-swellable di-acrylated Pluronic F127 (F127-DA), which showed higher mechanical strength than a conventional di-acrylated polyethylene glycol (PEG-DA) hydrogel. The uniform-sized vascular spheroids were spontaneously generated by human umbilical vein endothelial cells (HUVECs) and fibroblasts in the microwells. The endothelial functions of vascular spheroids were about 1-fold higher than those in two-dimensional (2D) culture, as indicated by secretion of nitric oxide (NO), prostacyclin (PGI2) and tissue factor pathway inhibitor (TFPI). Interestingly, the vascular spheroids with large diameter showed higher sensitivity to ethanol toxicity than those with small diameter, possibly due to the higher endothelial functions of large spheroids. Hence, F127-DA hydrogel with concave microwells provides a convenient way of forming uniform-sized spheroids that are useful for high throughput screening of drug/food toxicity.

1. Introduction

In vitro vascular models include two-dimensional (2D) monolayer culture on a plate, microfluidic vascular chips, and vascular spheroids. Among them, vascular spheroids are highly organized and do not require a perfusion system, so they show advantages in high-throughput study of compounds such as foods and drugs.[1,2]

There are several methods for preparing vascular spheroids. Non-adherent culture plates are most widely used to promote the spheroid formation,[3] while hanging drop is another method where the suspended cells in a droplet form one spheroid.[4,5] However, the size of the spheroids formed by these methods is uncontrollable and uneven.[6,7] By contrast, microfluidic devices that capture the cells inside the microchannels under perfusion can form uniform-sized spheroids,[8,9] but it is complex in construction and operation.

The hydrogel with concave microwells is the easiest method to form uniformly-sized spheroids in static culture,[10] where the size of microwells determined the diameter of spheroids.[11] Currently, various hydrogels such as di-acrylated polyethylene glycol (PEG-DA),[12–14] methacrylated gelatin (Gel-MA),[15,16] gelatin,[17] agarose[18] and chitosan[19] have been fabricated into hydrogel with microwells, but they have disadvantage on poor mechanical strength, causing the collapse and deformation of microwells. In addition, the cells are able to adhere on Gel-MA, gelatin, and chitosan, which makes the spheroids irregular.[15,17,19] Hence, high-strength and non-adherent hydrogel is required for fabrication of microwell patterns.

Pluronics are a class of biomedical polymers that are composed of PEG and poly(propylene oxide) (PPO) chains. They are widely used in cell culture and drug delivery for their non-toxic property,[20] and at the same time, most of Pluronics are non-adherent for cells due to the presence of non-fouling PEG chains.[21–23] In our previous study, we have prepared a non-swellable Pluronic F127-DA hydrogel which maintained the as-prepared size and mechanical strength after equilibrating at 37 °C in culture medium.[24] In this study, the F127-DA will be fabricated into hydrogel with concave microwells for the formation of vascular spheroids, while the conventional PEG-DA hydrogel is set as control. The effect of microwell diameters on spheroids size and functions will be investigated, and the impact of spheroid size on the ethanol toxicity is also evaluated.

2. Materials and methods

2.1. Chemicals

Pluronic F127, Sylgard 184 silicone elastomer kit (PDMS), acryloyl chloride, PEG (M_w 6000), dihydrorhodamine 123 (DHR123) and tetramethylazoazole blue (MTT) were purchased from Sigma-Aldrich (St. Louis, MO, USA). Fetal bovine serum (FBS), dimethyl sulfoxide (DMSO), phosphate buffered saline

College of Chemical and Biological Engineering, Zhejiang University, Hangzhou, 310027, China. E-mail: mengq@zju.edu.cn

† Electronic supplementary information (ESI) available. See DOI: 10.1039/d0ra06188c

(PBS), Dulbecco's modified Eagle's medium (DMEM) and antibiotic (penicillin–streptomycin) were ordered from Invitrogen (Grand Island, NY, US). Endothelial cell medium (ECM) was purchased from Science Cell (San Diego, Calif., USA). Iragacure 2959 were purchased from BASF (Florham Park, NJ, USA). Nitric oxide (NO) fluorometric assay kit was purchased from Biovision (Milpitas, CA, USA). Prostacyclin (PGI2), tissue factor pathway inhibitor (TFPI) and glutathione (GSH) ELISA kits were purchased from Chundu Bio. Co. (Wuhan, China). Bovine serum albumin (BSA), O. C. T compound, and trypsin-EDTA were purchased from Shanghai Biotech Engineering Co., Ltd. All other chemicals and reagents used in this study were of analytical grade and were obtained from Sinopharm Chemical Reagent Co. (Shanghai, China).

2.2. Preparation of the F127-DA and PEG-DA hydrogels with concave microwells

PEG-DA (M_W 6000) and F127-DA were synthesized according to the previously reported method.[25] The monomers with acylated degree over 90% were used for experiments. PEG-DA/F127-DA (10 wt%) were respectively dissolved in deionized water mixed with photoinitiator of Iragcure 2959 at 0.68 wt%. To fabricate the hydrogel with microwells, the three-dimensional (3D) printed resin molds (10 × 10 × 4 mm) were designed by Solid Works, which contained microwell arrays with a depth of 1 mm and diameters of 500–1000 μm (Fig. 1). Then PDMS soft templates were made by the 3D printed resin molds, and F127-DA or PEG-DA solution (10 wt%) was poured on the templates and cross-linked by UV light. After that, the hydrogels with microwells were peeled off from the PDMS templates and equilibrated in culture medium until use.

2.3. Detection on cell adhesion and protein adsorption on hydrogels

Human dermal fibroblasts (HF) were purchased from American type culture collection (ATCC) and cultured in DMEM containing 10% (v/v) FBS, 100 U mL^{-1} penicillin and 100 mg mL^{-1} streptomycin. Cells were seeded on the top of hydrogel surfaces at density of 1 $\times 10^5$ cells per cm.^{2} After 4 h of attachment, the unattached cells were carefully removed by rinsing with PBS and the adhered cells were lifted by trypsin-EDTA solution. The cell numbers were counted for triplicate samples using hemacytometer. The percent of attached cells was calculated as follows:

$$\%_{\text{attachment}} = \text{cells}_{\text{attached}}/\text{cells}_{\text{seeded}} \times 100\%$$

To detect the protein adsorption on the hydrogels, 0.3 g of each hydrogel was placed into PBS solution at 37 °C to equilibrate for 24 h. Then the hydrogels were transferred to 50 mL of PBS solution with BSA at 1 g L^{-1}. After shaking in a thermostatic oscillator at 37 °C for 24 h, the solution was sampled and residual BSA was measured by BCA protein assay kit.

2.4. Formation of vascular spheroids on the F127-DA hydrogel with microwells

Human umbilical vein endothelial cells (HUVECs) were purchased from ATCC and cultured in ECM supplemented with endothelial cell growth supplement (ECGS). The HUVECs and HFs (1 : 1) were seeded in the hexagon wells in the F127-DA hydrogels at a density of 1 × 10^6 cells per mL and grown as liquid overlay for 8 days. The culture medium was exchanged every two days.

To observe the distribution of the two cells in spheroids, the HUVECs were labeled by green fluorescence (CellTracker™ Green CMFDA, Invitrogen) while the HFs were labeled by red fluorescence (CellTracker CM-DiI, Invitrogen). The labeled HUVECs and HFs (1 : 1) were seeded in the hexagon wells in the F127-DA hydrogels at a density of 1 × 10^6 cells per mL and grown as liquid overlay for 8 days.

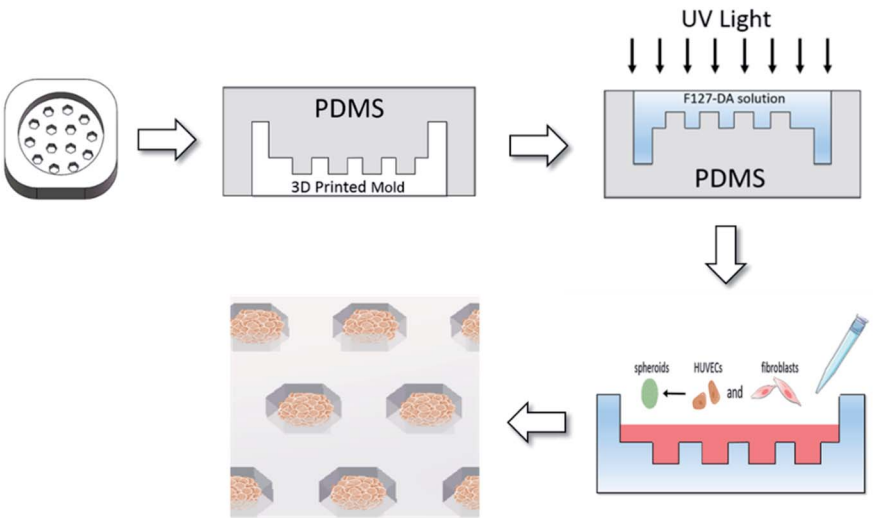

Fig. 1 Schematic depiction of the fabrication of hydrogel with concave microwells and formation of vascular spheroids.

2.5. Morphology observation and endothelial functions detection of vascular spheroids

Spheroids were fixed in 4% paraformaldehyde solution for 1 h, and embedded into O.C.T compound before frozen in −80 °C refrigerator. The spheroids were cut into sections with 10 μm thickness using a cryo-microtome, and the sections were stained by hematoxylin–eosin (H&E) staining.[26]

Endothelial functions were analyzed by measuring the concentration of NO, PGI2 and TFPI in culture medium at 2, 4, 6 and 8 days culture. NO was measured by detecting the accumulated nitrite (NO_2^-) in culture medium *via* the NO fluorometric assay kit.[27] PGI2 and TFPI contents were detected by the ELISA kits following the manufacturer's protocols.

2.6. Assessment of ethanol toxicity on vascular spheroids

After 48 hours of culture, the culture medium of vascular spheroids was changed to fresh medium containing 340 and 500 mM of ethanol. The control and ethanol groups were placed in different 24-well plates and sealed to prevent ethanol from volatilization for 48 h of incubation.

Cell viability was measured by MTT reduction. Briefly, 0.3 mg mL^{-1} MTT solution was added to the spheroids for incubating at 37 °C for 3 hours. Then, the solution was discarded, and HCl acidified isopropyl alcohol was added to the spheroids for 1 h of shaking at room temperature. The absorbance of solution was measured at 570 nm.

DHR123 was used to detect intracellular reactive oxygen species (ROS) in the spheroids. The spheroids were incubated with 10 μmol L^{-1} DHR123 in PBS at 37 °C for 30 minutes. After washing the cells with PBS for three times, the spheroids were detected under a fluorescent microplate reader at excitation/emission wavelength of 488/535 nm. For detection of GSH concentration, the spheroids were collected and analyzed by the colorimetric assay kit according to the instructions of manufacturer.[28]

2.7. Statistical analysis

All data from cell experiments were analyzed by means ± SD from three independent experiments. Comparisons between multiple groups were performed with the ANOVA test by SPSS, or results from two different groups were tested with the unpaired Student *t*-test. *P*-values less than 0.05 were considered statistically significant.

3. Result and discussion

3.1. Characterization of PEG-DA and F127-DA hydrogels

Swelling property is one of the inherent properties of hydrogels, which has been widely investigated to characterize water absorption and stability of biomaterials.[29] Fig. 2A exhibited the visual change of PEG-DA and F127-DA hydrogels after swelling with an obvious contrast in volume. PEG-DA hydrogel was swollen from 0.25 cm^3 to 0.9 cm^3 while no volume change was observed in F127-DA hydrogel (Fig. 2B). The "non-swellability" of F127-DA hydrogel at 37 °C have been characterized in detail in our previous study.[24] Since swelling property generally reduce the mechanical properties of hydrogels, the fracture strain and stress of PEG-DA hydrogel were much lower than F127-DA

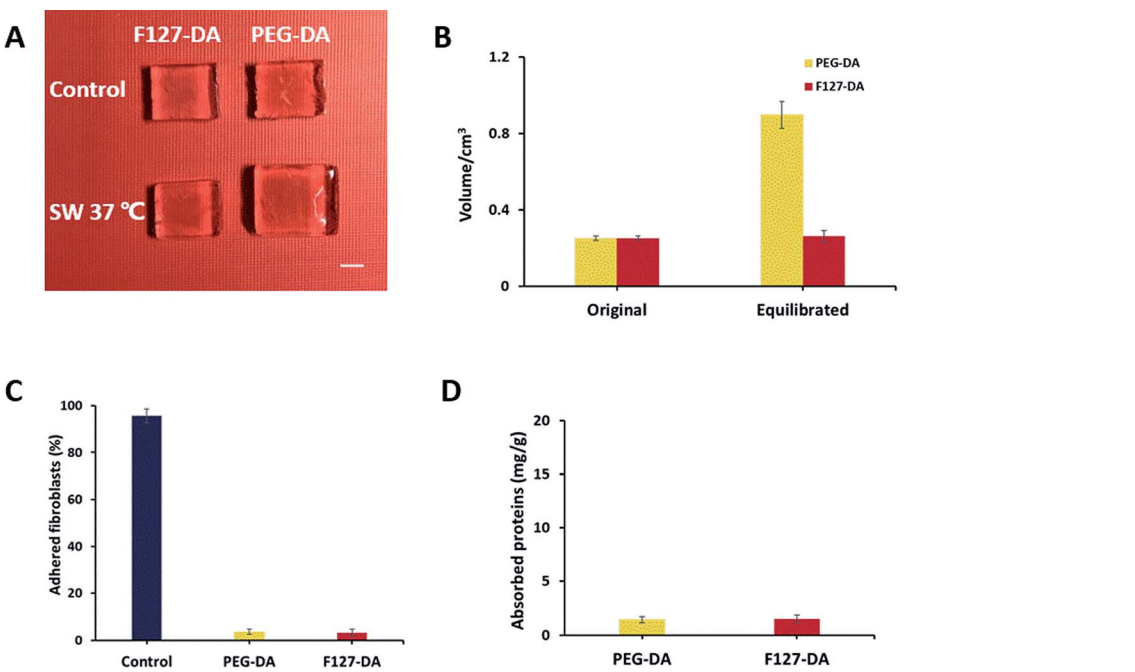

Fig. 2 Swelling property, cell adhesion and protein adsorption of di-acrylated polyethylene glycol (PEG-DA) and di-acrylated F127 (F127-DA) hydrogels in phosphate buffered saline (PBS) at 37 °C. (A) Photos of as-prepared and equilibrated hydrogels. Scale bar = 1 cm. (B) Volume change of as-prepared and equilibrated hydrogels. (C) Cell adhesion on the hydrogels. Control group is the tissue culture plate surface. (D) Bovine serum albumin (BSA) adsorption on the hydrogels.

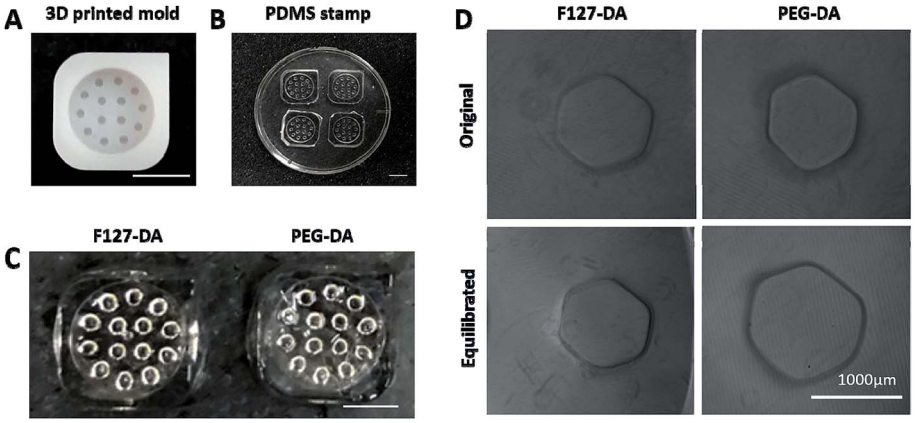

Fig. 3 Fabrication of hydrogels with concave microwells. (A) The three-dimensional (3D) printed resin mold. (B) The polydimethylsiloxane (PDMS) soft stamp. (C) As-prepared hydrogels with concave microwells. Scale bar = 5 mm. (D) Microwells of the as-prepared and equilibrated hydrogels. The F127-DA and PEG-DA hydrogels were observed under microscope (100×).

hydrogel (Fig. S1†), indicating that F127-DA hydrogel was stronger than PEG-DA hydrogel. Moreover, F127-DA hydrogels equilibrated in PBS at 37 °C for 24 h (F127-DA-eq) did not show any decline in mechanical properties while that of PEG-DA hydrogels equilibrated in PBS at 37 °C for 24 h (PEG-DA-eq) dropped sharply due to the swelling (Fig. S1†). Thus, the feature that F127-DA hydrogel showed a lower swelling ratio and higher compressive modulus was unique among numerous hydrogels.[30,31]

As the resistance of cell adhesion enables cells to aggregate spontaneously into spheroids, the adhesion of fibroblasts on the two hydrogels were detected.[32] It was found that the cells seeded on the two hydrogels did not show significant adhesion (Fig. 2C). In addition, the two hydrogels did adsorb little BSA as

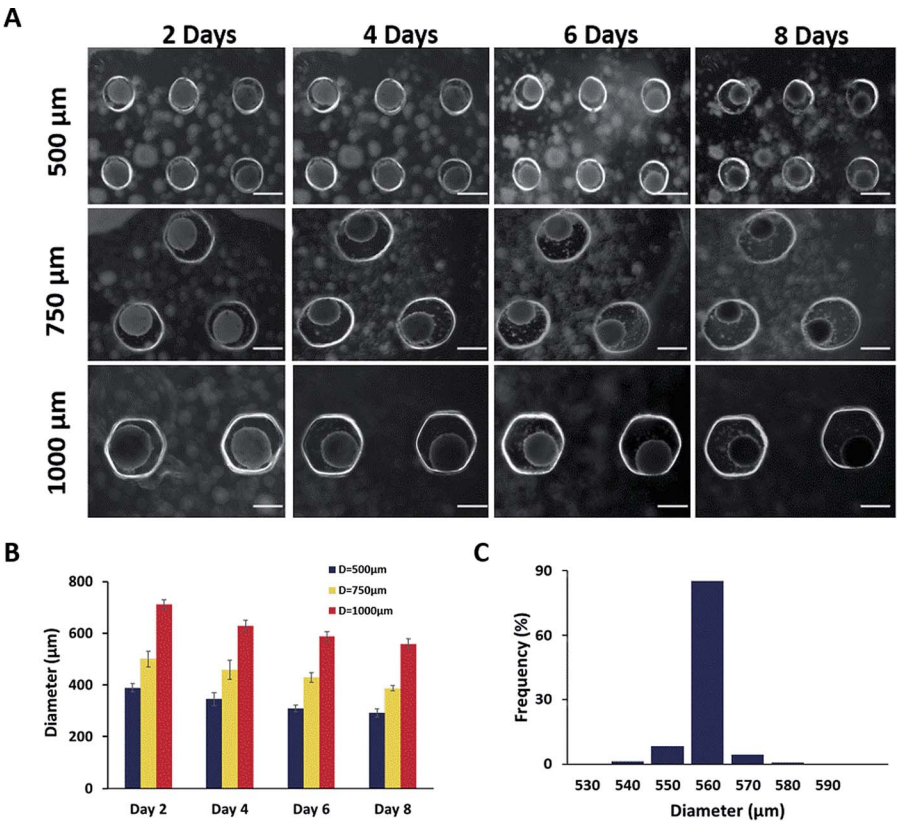

Fig. 4 Effect of concave diameter on spheroid size. (A) Phase-contrast images of spheroids created in concave with diameter of 500 μm, 750 μm, 1000 μm at day 2, 4, 6, 8. Scale bar = 500 μm. (B) The average diameter of spheroids cultured in 500 μm, 750 μm, 1000 μm concave microwells. (C) Size distribution of spheroids cultured in 1000 μm concave microwells after 8 days.

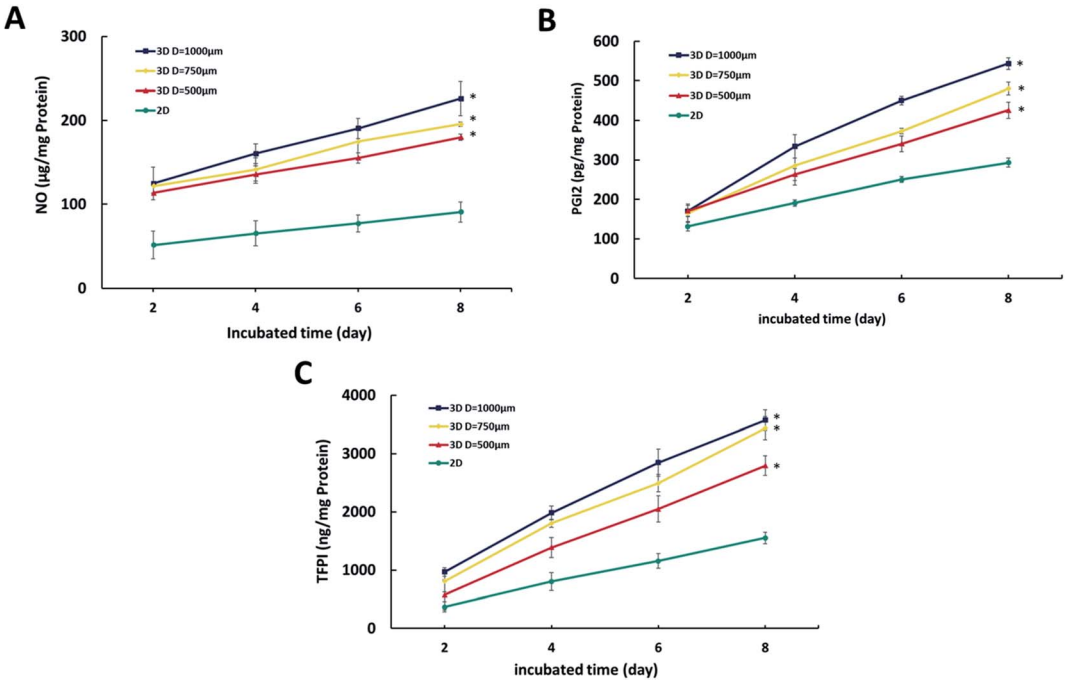

Fig. 5 Analysis of endothelial function of spheroids, measured as secretion of (A) nitric oxide (NO), (B) prostacyclin (PGI2) and (C) tissue factor pathway inhibitor (TFPI). *Significant difference ($p < 0.05$) from the 2D group.

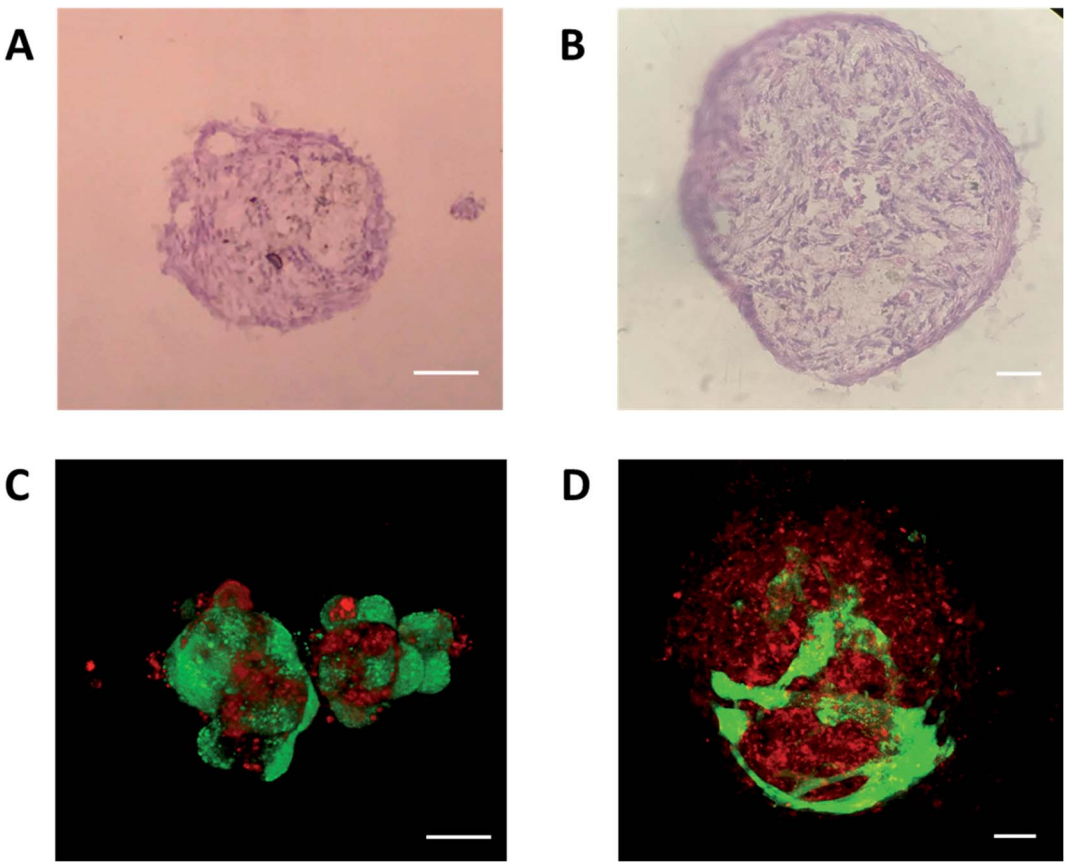

Fig. 6 Hematoxylin–eosin (H&E) staining of cryosectioned spheroids at day 8 in 500 μm (A) and 1000 μm (B) microwells. Confocal images of fluorescence staining at day 8 in 500 μm (C) and 1000 μm (D) microwells (green: HUVEC cells; red: fibroblasts). Scale bar = 100 μm.

well (Fig. 2D). By contrast, hydrogels made of natural materials such as chitosan and gelatin may form incomplete, irregular shaped and uneven sized spheroids due to their adhesion to cells.[17,19]

3.2. Fabrication of hydrogels with concave microwells

The 3D printed resin mold contained microwells with a depth of 1 mm and hexagonal circumcircle diameter of 200, 750 and 1000 μm (Fig. 3A). In order to record the position of each hole, the three corners of the mold were chamfered (Fig. 3A). Correspondingly, the PDMS soft stamp was obtained from the resin mold (Fig. 3B), while the F127-DA/PEG-DA hydrogels were formed under UV light on the PDMS stamps (Fig. 3C), respectively. Due to the non-swellable property of F127-DA hydrogel, the as-prepared size of microwells was well maintained at the equilibrated state, while the microwells on PEG-DA hydrogel expanded by 20% after swelling (Fig. 3D). Hence, the unexpected swelling of PEG-DA hydrogel caused the uncontrollable change on well diameters, which was unfavorable for the culture of vascular spheroids.

3.3. Effect of microwell sizes on spheroid morphology and functions

The HUVEC and HF in the microwells spontaneously gathered together to form spheroids in the first 2 days (Fig. 4A). As time went on, the spheroids became smaller since the cells stuck to each other more compactly. As shown in Fig. 4B, the average diameter of spheroids in 500, 750 and 1000 μm of microwells were approximately 380, 500 and 700 μm at day 2, and gradually decreased to 300, 380 and 560 μm at day 8 due to the presence of fibroblasts which secret collagen to promote the spheroid formation.[33] After 8 days culture, the spheroids were uniform in diameters with a narrow distribution (Fig. 4C).

Next, endothelial functions were evaluated by measuring NO, PGI2 and TFPI. NO is a major endothelial-derived relaxing factor,[34] and PGI2 and TFPI are important cytokines produced by endothelial cells.[35,36] As shown in Fig. 5, cumulative secretion of NO, PGI2 and TFPI of spheroids in whatever size was higher than the 2D co-culture, indicating the maintained endothelial functions and phenotypes in the hydrogel microwells. Moreover, as the diameter of spheroids increased, the endothelial functions were also enhanced.

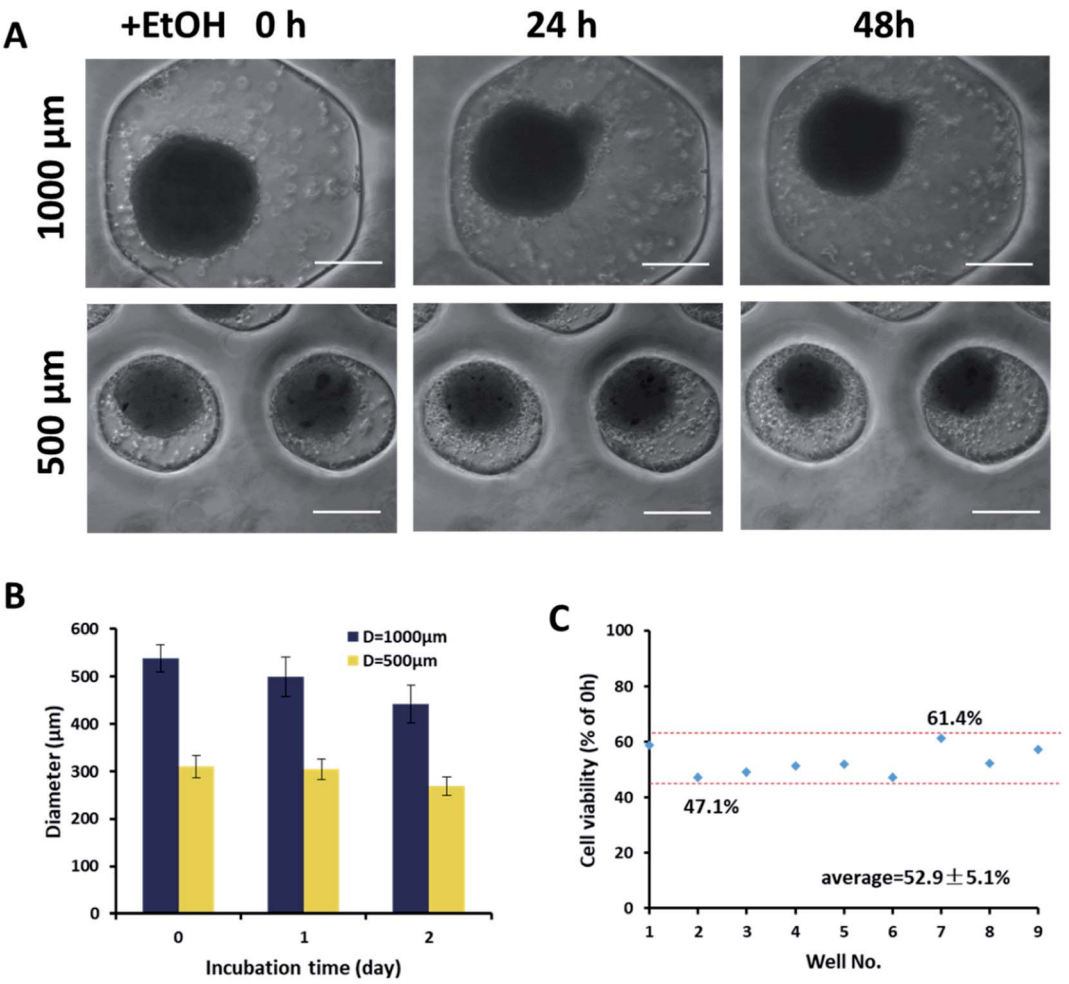

Fig. 7 Response of vascular spheroids to ethanol toxicity. (A) Images of spheroids exposed to ethanol at 340 mM for 24 and 48 h in concave with diameter of 500 and 1000 μm. Scale bar = 300 μm. (B) The average diameter analysis of spheroids exposed to ethanol for 1, and 2 days. (C) Cell viability of nine spheroids exposed to ethanol in 1000 μm concave microwells after 2 days.

In order to analyze the internal structure of vascular spheroids, H&E and fluorescent staining was carried out on the spheroids at day 8 in 500 and 1000 μm microwells. As shown in Fig. 6A and B, H&E staining of sectioned spheroids revealed a compact, uniform structure with a smooth perimeter and no signs of central apoptosis or necrosis. Among the large spheroids, HUVECs migrated to the surface of spheroids and formed a tubular network structure (Fig. 6D), which was consistent with previous reports that a vascular network formed at the edges of the vascular spheroids.[37] However, HUVECs were still dispersedly distributed on the surface of the small spheroids without a tubular network structure. This difference on structure might result in the higher endothelial functions in large spheroids.

3.4. Response of vascular spheroids to ethanol vascular toxicity

Because the size of vascular spheroids had a significant impact on vascular function, it may also lead to differences in the response to toxicity. To illustrate the importance and necessity of the size uniformity of the spheroid in the toxicity evaluation, the ethanol toxicity on different sized spheroid was further investigated. As a common vascular toxic substance, ethanol induced cells to produce ROS which caused lipid peroxidation of the cell membrane and resulted in the decrease of GSH.[38]

Fig. 7A showed the morphological changes of two sizes of spheroids after being exposed to ethanol at 340 mM for 24 and 48 h. With the increase of exposure time, the edges of spheroids became rough, and the single cells dropped off from the spheroids. After 48 h of culture, the diameter of large spheroids decreased by 17%, while that of small spheroids decreased by only 10% (Fig. 7B), which indicated that large spheroids were more sensitive to ethanol toxicity. This might be caused by the higher endothelial functions of the large spheroids rather than the difference in mass transfer, since the smaller spheroids should perform better mass transfer. For the uniform in size of spheroids, cell viability of nine spheroids from different microwells of 1000 μm was only about ±5% after exposed to the same ethanol concentration for 48 h (Fig. 7C).

Next, the spheroids with different sizes were treated by ethanol at 340 and 500 mM for 48 h, while the cell viability, NO, ROS and GSH was evaluated. With the increase of ethanol concentration, the cell viability of large spheroids eventually dropped to about 50%, while the cell viability of the small spheroids eventually exceeded 80% (Fig. 8A). It indicated the fact that large spheroids were more sensitive to ethanol toxicity, consisted with the observation in Fig. 7A. The increase of ethanol concentration also increased the ROS levels and decreased NO/GSH levels of both sizes of spheroids. The negative correlation between ROS and NO/GSH was reasonable

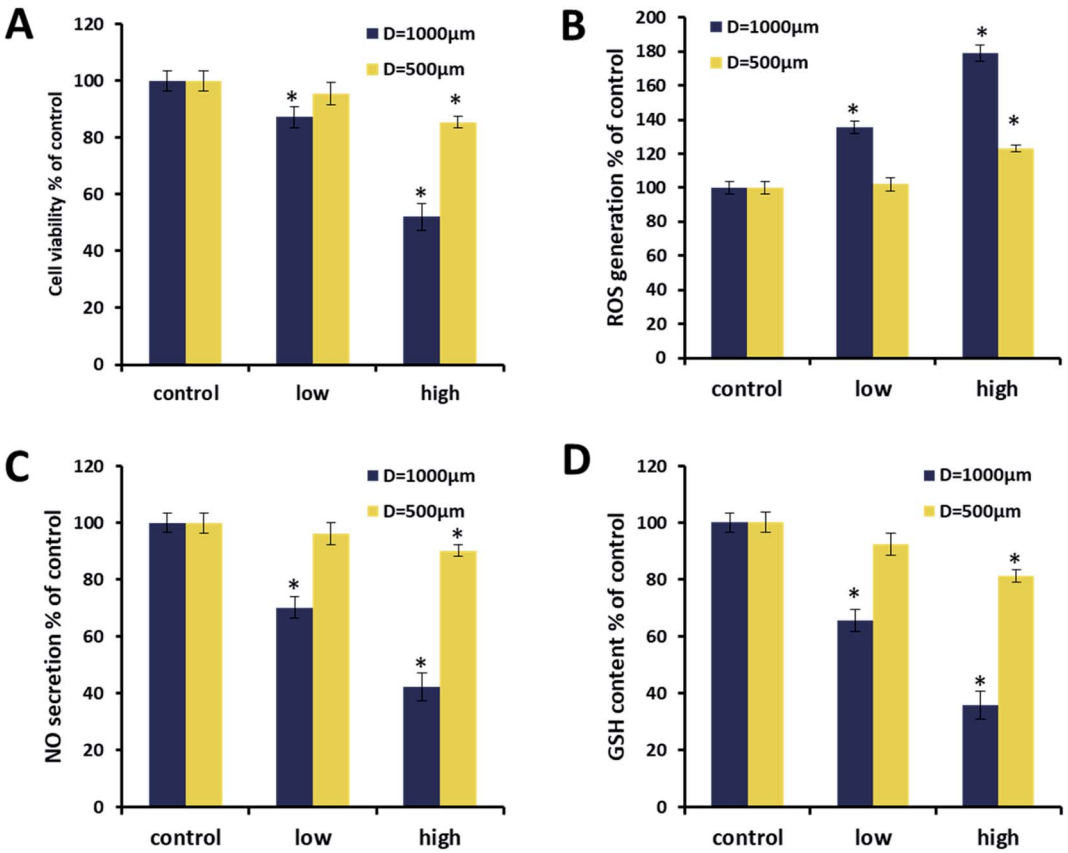

Fig. 8 Vascular toxicity of two ethanol concentrations (340 and 500 mM) to spheroids with different sizes, measured by secretion of (A) cell viability, (B) nitric oxide (NO), (C) reactive oxygen species (ROS) and (D) glutathione (GSH). *Significant difference ($p < 0.05$) from control group.

because ROS induced by ethanol can reduce NO content through the formation of peroxynitrite[39] and it also impaired the content of GSH.[38] The three indicators in larger spheroids were more significantly changed than those of the smaller spheroids, confirming the conclusion that larger spheroids were more sensitive to ethanol toxicity.

Hence, our results indicated the role of spheroid sizes on chemical toxicity such as ethanol. As most of vascular spheroids are not uniform in size,[3,7,40] they may not suitable for toxic evaluation due to the impaired reliability. By contrast, the spheroids in F127-DA hydrogel with microwells were size-controllable, which provided a model *in vitro* for toxicity assessment.

4. Conclusions

In this study, we have fabricated a F127-DA hydrogel with microwells for formation of vascular spheroid, since F127-DA hydrogel was non-swellable, mechanical strong, and non-adhesive for cells. The uniform-sized vascular spheroids were spontaneously generated by HUVEC and fibroblasts in the microwells. The endothelial functions of vascular spheroids were about 1-fold higher than those in 2D culture, as indicated by measurement of NO, PGI2 and TFPI. Interestingly, the vascular spheroids with large diameter showed higher sensitivity to ethanol toxicity than those with small diameter, possibly due to the higher endothelial functions of large spheroids. Hence, F127-DA hydrogel with concave microwells provides a convenient way for formation of uniform-sized spheroids that are useful for high throughput screening of drug/food toxicity.

Conflicts of interest

There are no conflicts to declare.

References

1 E. Fennema, N. Rivron, J. Rouwkema, C. van Blitterswijk and J. de Boer, *Trends Biotechnol.*, 2013, **31**, 108–115.
2 M. W. Laschke and M. D. Menger, *Trends Biotechnol.*, 2017, **35**, 133–144.
3 N. Dorst, M. Oberringer, U. Grässer, T. Pohlemann and W. Metzger, *Ann. Anat.*, 2014, **196**, 303–311.
4 Y. Nashimoto, T. Hayashi, I. Kunita, A. Nakamasu, Y.-s. Torisawa, M. Nakayama, H. Takigawa-Imamura, H. Kotera, K. Nishiyama and T. Miura, *Integr. Biol.*, 2017, **9**, 506–518.
5 S. Brouillet, P. Hoffmann, M. Benharouga, A. Salomon, J.-P. Schaal, J.-J. Feige and N. Alfaidy, *Mol. Biol. Cell*, 2010, **21**, 2832–2843.
6 S.-h. Hsu, T.-T. Ho, N.-C. Huang, C.-L. Yao, L.-H. Peng and N.-T. Dai, *Biomaterials*, 2014, **35**, 7295–7307.
7 T. Korff and H. G. Augustin, *J. Cell Biol.*, 1998, **143**, 1341–1352.
8 B. Patra, Y.-S. Peng, C.-C. Peng, W.-H. Liao, Y.-A. Chen, K.-H. Lin, Y.-C. Tung and C.-H. Lee, *Biomicrofluidics*, 2014, **8**, 052109.
9 H. Ota, T. Kodama and N. Miki, *Biomicrofluidics*, 2011, **5**, 034105.
10 F. Brandl, F. Sommer and A. Goepferich, *Biomaterials*, 2007, **28**, 134–146.
11 F. Ruedinger, A. Lavrentieva, C. Blume, I. Pepelanova and T. Scheper, *Appl. Microbiol. Biotechnol.*, 2015, **99**, 623–636.
12 K. C. Hribar, D. Finlay, X. Ma, X. Qu, M. G. Ondeck, P. H. Chung, F. Zanella, A. J. Engler, F. Sheikh and K. Vuori, *Lab Chip*, 2015, **15**, 2412–2418.
13 M. Singh, D. A. Close, S. Mukundan, P. A. Johnston and S. Sant, *Assay Drug Dev. Technol.*, 2015, **13**, 570–583.
14 J. M. Lee, L. Yang, E.-J. Kim, C. D. Ahrberg, K.-B. Lee and B. G. Chung, *Sci. Rep.*, 2018, **8**, 1–10.
15 J. Casey, X. Yue, T. D. Nguyen, A. Acun, V. R. Zellmer, S. Zhang and P. Zorlutuna, *Biomed. Mater.*, 2017, **12**, 025009.
16 X. Yue, T. D. Nguyen, V. Zellmer, S. Zhang and P. Zorlutuna, *Biomaterials*, 2018, **170**, 37–48.
17 C. S. Shin, B. Kwak, B. Han and K. Park, *Mol. Pharmaceutics*, 2013, **10**, 2167–2175.
18 A. R. Thomsen, C. Aldrian, P. Bronsert, Y. Thomann, N. Nanko, N. Melin, G. Rücker, M. Follo, A. L. Grosu and G. Niedermann, *Lab-on-a-Chip*, 2018, **18**, 179–189.
19 J. Fukuda, A. Khademhosseini, Y. Yeo, X. Yang, J. Yeh, G. Eng, J. Blumling, C.-F. Wang, D. S. Kohane and R. Langer, *Biomaterials*, 2006, **27**, 5259–5267.
20 X. L. Li, R. R. Fan, Y. L. Wang, M. Wu, A. P. Tong, J. Shi, M. L. Xiang, L. X. Zhou and G. Guo, *RSC Adv.*, 2015, **5**, 101494–101506.
21 L. Benning, L. Gutzweiler, K. TroNdle, J. Riba, R. Zengerle, P. Koltay, S. Zimmermann, G. B. R. Stark and G. Finkenzeller, *J. Biomed. Mater. Res., Part A*, 2018, **106**, 935–947.
22 S. H. Oh, J. G. Kang and J. H. Lee, *J. Biomed. Mater. Res., Part B*, 2018, **106**, 172–182.
23 D. E. Heath, A. R. M. Sharif, C. P. Ng, M. G. Rhoads, L. G. Griffith, P. T. Hammond and M. B. Chan-Park, *Lab Chip*, 2015, **15**, 2073–2089.
24 C. Shen, Y. Li, Y. Wang and Q. Meng, *Lab Chip*, 2019, **19**, 3962–3973.
25 A. Sosnik, D. Cohn, J. S. Román and G. A. Abraham, *J. Biomater. Sci., Polym. Ed.*, 2003, **14**, 227–239.
26 H. Colley, V. Hearnden, A. Jones, P. Weinreb, S. Violette, S. Macneil, M. Thornhill and C. Murdoch, *Br. J. Cancer*, 2011, **105**, 1582–1592.
27 P. Damiani and G. Burini, *Talanta*, 1986, **33**, 649–652.
28 A. M. Smith, D. R. Zeve, J. J. Grisel and W.-J. A. Chen, *Dev. Brain Res.*, 2005, **160**, 231–238.
29 H. T. Peng, M. Mok, L. Martineau and P. N. Shek, *J. Mater. Sci.: Mater. Med.*, 2007, **18**, 1025–1035.
30 J. W. Nichol, S. T. Koshy, H. Bae, C. M. Hwang, S. Yamanlar and A. Khademhosseini, *Biomaterials*, 2010, **31**, 5536–5544.
31 Q. Xing, K. Yates, C. Vogt, Z. Qian, M. C. Frost and F. Zhao, *Sci. Rep.*, 2014, **4**, 4706.

32 J. Thiele, Y. Ma, S. M. C. Bruekers, S. Ma and W. T. S. Huck, *Adv. Mater.*, 2014, **26**, 125–148.
33 A. S. Narayanan, R. Page and J. Swanson, *Biochem. J.*, 1989, **260**, 463–469.
34 L. Gliemann, M. Nyberg and Y. Hellsten, *Free Radical Res.*, 2014, **48**, 71–83.
35 R. J. Gryglewski, in *The Prostaglandin System*, Springer, 1981, pp. 73–84.
36 A. Dahm, F. R. Rosendaal, T. O. Andersen and P. M. Sandset, *Br. J. Haematol.*, 2006, **132**, 333–338.
37 D. Rogozhnikov, P. J. O'Brien, S. Elahipanah and M. N. Yousaf, *Sci. Rep.*, 2016, **6**, 39806.
38 G. Addolorato, L. Leggio, V. Ojetti, E. Capristo, G. Gasbarrini and A. Gasbarrini, *Appetite*, 2008, **50**, 50–56.
39 L. K. Ng, M. Hupé, J. Harnois and D. Moccia, *J. Sci. Food Agric.*, 1996, **70**, 380–388.
40 T. Hayashi, H. Takigawa-Imamura, K. Nishiyama, H. Shintaku, H. Kotera, T. Miura and R. Yokokawa, *2015 28th IEEE International Conference on Micro Electro Mechanical Systems (MEMS)*, 2015, pp. 476-479.

